ORIGINAL PAPER

EXPERIMENTAL RESEARCH CONCERNING WATERSIDE CORROSION OF FUEL CLADDING IN CANDU REACTOR

DUMITRA LUCAN[1,2]

Manuscript received: 10.11.2023; Accepted paper: 14.01.2024;
Published online: 30.03.2024.

Abstract. *Zirconium alloy (Zircaloy-4) is widely used for fuel cladding in the Canadian Deuterium Uranium (CANDU) heavy water reactors. However, degradation due to waterside corrosion can limit the in-reactor design life of the nuclear fuel. For this reason, efforts must be made to understand the mechanisms of corrosion and to mitigate its effects. The purpose of the experimental research related to this work consists of the assessment of corrosion of the CANDU fuel cladding material. The paper presents the results obtained by in-situ monitoring of the Pressurized Heavy Water Reactor (PHWR) water chemistry effect on fuel cladding corrosion, Zircaloy-4. Optical metallographic and Scanning Electron Microscopies (SEM), as well as X-ray diffraction (XRD) analysis, were used to evaluate the corrosion behavior of the fuel cladding material, Zircaloy-4 coupons, exposed in a Primary Heat Transport System (PHTS) autoclave system. The obtained results are useful for characterizing the corrosion behavior of Zircaloy-4 coupons exposed in the autoclave system at Cernavoda NPP for long periods.*

Keywords: *Zircaloy-4; fuel cladding; PHTS; water chemistry; corrosion.*

1. INTRODUCTION

The use of zirconium alloys as cladding materials is based on the excellent behavior of zirconium alloys under normal operating conditions as well as the significant advantage of neutron economy. However, in the event of severe accidents, the use of zirconium alloys can be a major disadvantage. The Fukushima Daiichi Nuclear Plant accident brought challenges to the nuclear industry and renewed attention to the idea of Accident-Tolerant Fuels (ATFs). These materials have higher resistance to core degradation, lower oxidation kinetics, and can withstand high temperatures for a longer duration of time [1,2]. For the development and qualification of these materials, it is desirable to benefit from the experience gained in the field of cladding materials used in the present and the lessons learned from the research programs carried out so far.

Water chemistry control in Nuclear Power Plants (NPPs) is important for structural material integrity, plant radiation levels, deposit build-up, and safety. One of the most important NPP systems is the Primary Heat Transport System (PHTS), which plays a role in active zone cooling and heat transfer to steam generators. In PHTS, chemical control is directed to keep chemical parameters within specified limits to mitigate the corrosion of the key equipment and related piping, to control the corrosion rate and impurity concentration, such as corrosion and fission products, and to minimize activity transport and heat transfer surface fouling.

[1] Institute for Nuclear Research, 115400 Mioveni, Romania.
[2] Technical Sciences Academy of Romania, 030167 Bucharest, Romania. E-mail: dida.lucan@gmail.com.

https://doi.org/10.46939/J.Sci.Arts-24.1-b03

By operating in an aqueous environment at high temperatures and pressure, the structural materials from the PHTS are covered with protective oxide films, which maintain the corrosion rate at admissible limits. Many potential factors, can degrade the protective films and consequently intensify the corrosion processes. To minimize these adverse effects, an optimal water chemistry control and corrosion-monitoring program must be applied, [3,4].

The understanding of the corrosion degradation phenomena that result in the failure of some components from PHTS of CANDU NPP necessitates investigation of the structural materials corrosion processes in different conditions of water chemistry and temperature. Water chemistry management in Nuclear Power Plants can then be applied to mitigate the corrosive environments inherent in plant operation.

The basis of the chemistry control process consists of operational experience, laboratory tests, structural material corrosion behavior, and transport and deposition of impurities and corrosion products under operating conditions, [5,6].

The precipitation of crud deposits in the core must be avoided as much as possible, as it can lead to fouling of the fuel, loss of heat transfer efficiency, fuel failures, increased radiation fields, and neutronic disturbances in the core. The deposition rate on the surfaces is controlled by the concentration of impurities in the coolant, pH of the water, and surface temperature. To prevent cladding failures, the coolant chemistry must be monitored and controlled to reduce the amount of deposited crud and the oxygen potential [7-9].

The PHTS from Cernavoda Unit#1 NPP is arranged in two separate loops, which are normally tied together with each loop serving 190 fuel channels, comprising two boilers, two circulating pumps, two reactor inlet headers, two reactor outlet headers, and the necessary interconnecting piping. The chemical Control and Diagnostic Parameters for steady-state operation are summarized in Table 1 [10].

Table 1. Chemical control and diagnostic parameters specification.

Parameter	**Sample Origin**	**Specification**	**Desired Value**
pH	Main System IX* Outlet	10.2-10.8 NIA	10.2-10.4 IX inlet
Dissolved D_2 [mL/kg]	Main System	3-10	7
Chloride [mg/kg]	Main System IX* Outlet	≤ 0.2 < IX inlet	ALARA** ALARA
I-131 MBq/kg	Main System IX* Outlet	< 500 < IX inlet	ALARA ALARA
D_2 [%by vol.]	Storage tank cover gas	≤ 2	ALARA
O_2 [% by vol.]	Storage tank cover gas	≤ 1	ALARA
N_2 [% by vol.]	Storage tank cover gas	≤ 6	ALARA
Lithium [mg/kg]	Main System	0.4-1.1	0.5
Conductivity [μS/cm]	Main System	8-25	8-20
Fluoride [mg/kg]	Main System IX* Outlet	< 0.1 < IX inlet	ALARA ALARA
Suspended Solids [mg/kg]	Main System Gland Seal	< 0.1 < 0.010	ALARA ALARA
Total Organic Carbon [mg/kg]	Main System	≤ 1.0	ALARA
Radionuclide Gama Scan [MBq/L]	Main System IX* Outlet	0.1 < IX inlet	ALARA ALARA

** IX – ions exchanger; **ALARA – As Low as Reasonably Achievable*

Chemical control of the PHT System and Auxiliaries is required to minimize the corrosion of the system components, limit the production rate of radioactive corrosion products, minimize the fouling of the heat transfer surfaces by controlling the crud movement

and removal, and maintain the heat transport storage tank cover gas deuterium and oxygen concentrations below explosive limits.

The above objectives were achieved by controlling the pH in the range of 10.1 to 10.4, maintaining excess dissolved deuterium in the range of 3-10 mL/kg to scavenge oxygen, maintaining the purity of the PHT heavy water via the purification loop, which contains Li^+/OD^- ion exchange resin, and purging the heat transport storage tank cover gas when required.

2. EXPERIMENTAL

The process of corrosion products formation on the Zircaloy-4 fuel cladding surface and its consequences were evidenced by performing experiments in autoclave circuits assembled in a by-pass loop of a CANDU-6 Reactor at NPP Cernavoda and in laboratory static autoclaves. The formation of corrosion products on the fuel cladding surface during steady-state operation was followed by exposure of Zircaloy-4 coupons in autoclave circuits assembled in a by-pass loop of the CANDU-6 Reactor at NPP Cernavoda. The chemical conditions for autoclaving circuits were standard conditions for the reactor, which comply with the chemical control and diagnostic parameters for steady-state operation of the CANDU-6 Reactor [10].

To investigate the corrosion process of some structural materials from the Primary Heat Transport System of the CANDU 6 reactor, corrosion experiments were performed in autoclaves assembled in by-pass loops of the CANDU 6 reactor PHTS Cernavoda Unit#1.

To assist in the monitoring and optimization of chemistry control and provide warnings of serious corrosion and/or activity transport conditions, an Autoclave System flow diagram is provided. The Autoclave System consists of four autoclave circuits, one from the reactor outlet header to the boilers and one from the circulating pump to the reactor inlet header, on each of the two PHT loops, Fig. 1 [10].

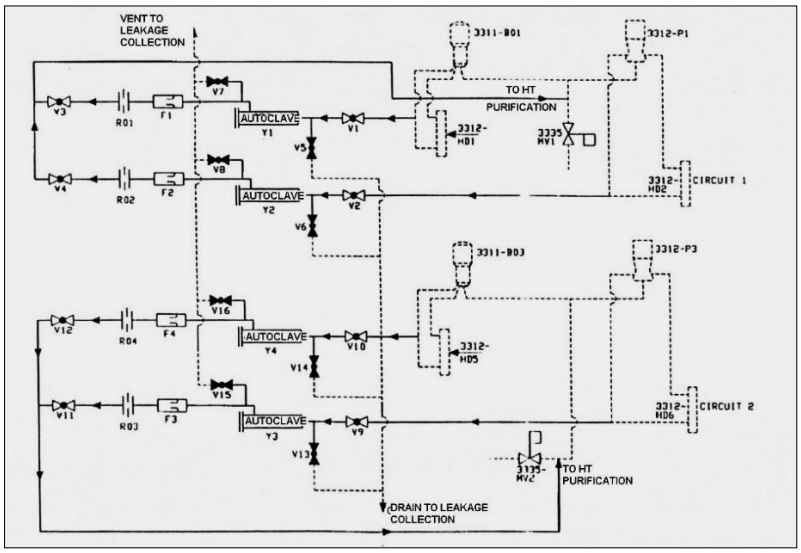

Figure 1. PHTS autoclave system diagram.

The corrosion product formation on the fuel cladding surface during steady state operation was followed by the removal of Zircaloy-4 coupons from autoclave circuits assembled in a bypass loop of the CANDU-6 Reactor at NPP Cernavoda. The chemical

conditions for the autoclave circuits were established following standard procedures for the reactor and were designed to meet the chemical control and diagnostic parameters required for the steady-state operation of the CANDU-6 Reactor.

In normal operation, the restriction orifices should maintain a flow of approximately $250g*s^{-1}$ to achieve a flow rate of approximately 4.7 $m*s^{-1}$. Each autoclave contained six hanger bars numbered 1 to 6 (S1-S6).

Standard coupons were 30 mm × 15 mm with a thickness between 1.0 and 1.5 mm. Coupons were mounted in pairs, with a maximum of 6 pairs or 12 coupons per hanger bar and 72 coupons in all. Each hanger bar (S1-S6) from the four autoclaves (Y1-Y4) contained Heat Transport System (HTS) materials as follows: carbon steel ASTM A 106 grade B and ASTM A 516 piping, headers, feeders, heat exchanger shell, stainless steel 403 m (end fittings) and 304 L (tubing of heat exchangers), Zr-2.5% Nb (pressure tube), Incoloy 800 (tubing of steam generators), and Zircaloy-4 (fuel cladding).

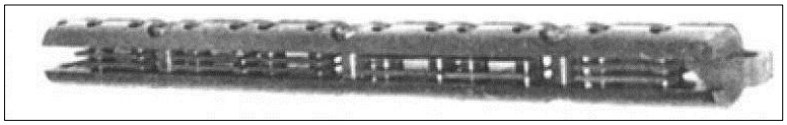

Figure 2. The coupons hanger bar.

The chemical compositions of the coupons from Zircaloy-4 must meet the ASME chemical composition requirements presented in Table 2.

Table 2. Chemical composition (% massic) of Zircaloy-4 cladding (ASME).

Alloy	UNS#	Sn	Fe	Cr	Ni	O [ppm]	Hf [ppm]
Zy-4	R60804	1.2-1.7	0.18-0.24	0.07-0.13	0.03-0.08	1200-1400	100

The corrosion coupons, from Zircaloy-4, used in this work were parallelepiped with dimensions of 15 × 10 × 2 mm. Before testing, the coupons were polished with grit paper and cleaned ultrasonically. Initially, the coupons were passivized in a LiOH solution with Na_2EDTA (142 hours at 150^0C and 47 hours at 260^0C) in static autoclaves or during the commissioning of the primary circuit of the CANDU 6 reactor. The investigated coupons were as follows: Y2 – 77 – exposure time <5 years (approximately 1440 days) and Y3-259 – exposure time> 5 years (approximately 2520 days).

The destructive examinations included cutting the transverse cross sections of the cladding for metallographic examinations. These examinations were performed to measure the thickness of the crud and determine the effect of these deposits on the corrosion of fuel cladding materials. The quantity of the adherent corrosion products was dependent on the thickness, especially the physicochemical characteristics of the initial zirconium oxide films. To confirm this, as well as the impact of corrosive deposit on Zircaloy-4 alloy oxidation and hydriding, many laboratory experiments have been performed in static autoclaves at different temperatures on Zircaloy-4 coupons, used in PHWR systems [11].

After in-situ testing, analysis of the corrosive deposits, oxidation, and hydriding of the Zircaloy-4 coupons was performed using gravimetric analysis, metallographic and electronic microscopy examinations, and X-ray diffraction analysis. The weight modifications due to oxidation were measured using a SHIMADZU AUW 220 analytical balance (Shimadzu, Japan) providing a precision of ±0.01 mg. The surface morphologies and the cross sections of the corrosion samples were analyzed with the optical microscope OLYMPUS GX 71 equipped with the "autoSYS auto" analysis program (Olympus Corporation, Tokyo, Japan) and scanning electron microscope TESCAN VEGA II LMU type (Tescan Group, Czech

Republic. X-ray diffraction system, Analytical X'Pert PRO MPD (Malvern Panalytical Ltd, United Kingdom), was also used for tested coupon characterization.

To determine the thickness of the oxide layer, small pieces were cut from the coupons and wrapped in copper foil, embedded in conductive cupric resin, and ground (P #4000 _m). The hydrides were highlighted by chemical etching in a solution composed of 45 mL HNO_3 (67%), 45 mL H_2O_2 (30%), and 7 mL HF (30%) for 20 s.

3. RESULTS AND DISCUSSION

Corrosive deposits formed on the fuel claddings during the steady-state operation of the CANDU reactor are presented in Fig. 3.

Figure 3. The aspect of coupons observed by visual examination.

The surfaces of the coupons were examined visually at low magnification or with a magnifying glass at 12X magnification to identify any defects due to corrosion. This analysis provides the first estimate of the state of the surfaces of the different components in the boiler. Upon visual examination of the Zircaloy-4 coupons, no differences were found between the two coupons in terms of the surfaces of the formed oxides. The coupons had no visible pores or cracks on their surface.

Both coupons had a surface completely covered with glossy black oxide. The oxide that forms on the zirconium alloys has a white color if the oxide is stoichiometric ZrO_2, and the color black or grey is specific to a non-stoichiometric oxide ZrO_{2-x}, adherent, or protective. It is expected that the oxide layer will have a small thickness and be uniform. The values of crud thus obtained are in agreement with theories that explain the mechanism of generation of corrosion products in CANDU reactors with carbon steel feeders. The coupons from the inlet reactor autoclaves (260°C) have larger deposits because the coolant is probably still supersaturated in iron concerning the solubility value and present a larger percentage (60%) of adherent crude deposited on the surface. The coupons inserted in the outlet reactor autoclaves (310^oC) showed smaller values of total deposits and a smaller percentage of adherent crud (30%), which can be attributed to the presence of particulate matter formed by the erosion of recently precipitated crystals. In the case of tested coupons for 2520 days, the corrosion rate, determined by gravimetric analysis, was approximately 0.276–0.313μm/dm^2.day.

3.1. OPTICAL MICROSCOPY ZIRCALOY-4 MORPHOLOGY ANALYSIS

The surface morphology of coupon Y2-77, exposed for <5 years, Figure 4 (x200), shows an adherent, glossy, black film with pink irises. The surface morphology of coupon Y3-259, exposed for >5 years, Fig. 5 (x200), shows a film adherent, glossy, black with dark grey.

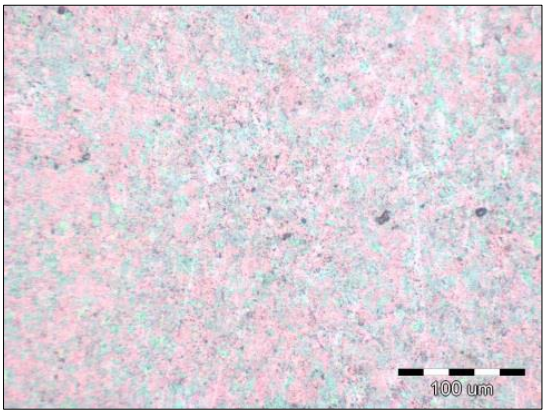

Figure 4. Zy-4_Y2-77_<5 years_(x200).

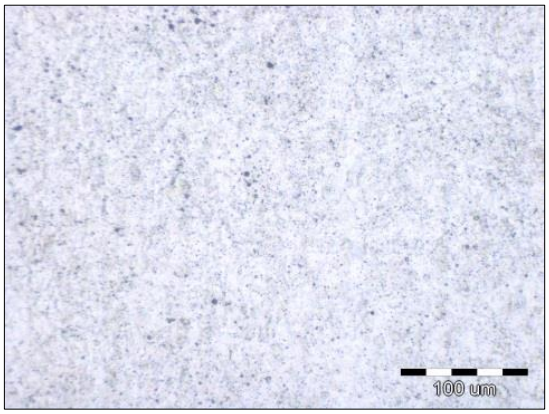

Figure 5. Zy-4_Y3-259_>5 years_(x200).

3.2. OPTICAL MICROSCOPY ZIRCALOY-4 THICKNESS LAYER ANALYSIS

The layer thickness was measured automatically at various magnifications (x200–x1000). In Table 3, the thickness of the oxide layer is presented, and in Figs. 6 and 7, the aspect of the oxide layer for each coupon is analyzed.

Table 3. The thickness of the oxide layer.

Zy-4	Y2-77	< 5 years	1.4-2.4μm	1.8μm
	Y3-259	> 5 years	2.3-3.3μm	2.6μm

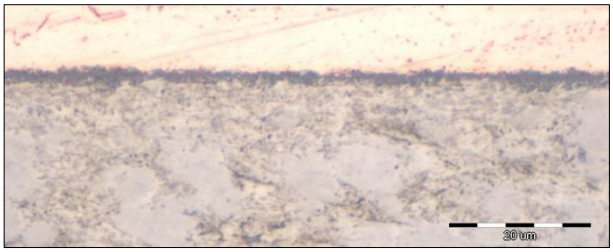

Figure 6. Zy-4 Y2-77.

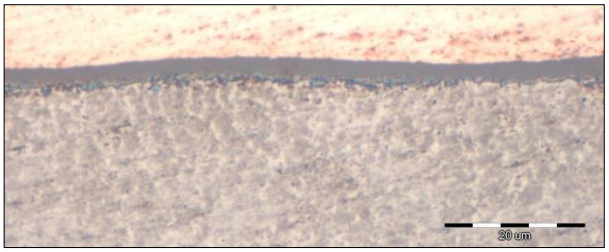

Figure 7. Zy-4 Y3-259.

The thickness of the oxide layer formed on the Zircaloy-4 coupon after 1440 days of exposure in the PHTS autoclave system is located in the range of 1.4-2.4 μm and after 2520 is approximately 2.6 μm.

The oxide layer on the Y3-259 coupon (autoclaved over 5 years, Fig. 7) was approximately 1.5 times thicker than that on the Y2-77 coupon (autoclaved under 5 years, Fig. 6).

3.3. OPTICAL MICROSCOPY ZIRCALOY-4 MICROSTRUCTURE ANALYSIS

The microstructures of the control sample (as received) and Zircaloy-4 coupons show Zirconium alpha hydrides (αZr) as can be seen in Fig. 8 (x100) and Fig. 9 (x200) – control of Zircaloy-4 (sheath): hydrides; Fig. 10 (x100) and Fig. 11 (x200) – coupon Y2-77, <5 years: hydrides; Fig. 12 (x100) and Fig. 13 (x200) – coupon Y3-259, > 5 years: hydrides.

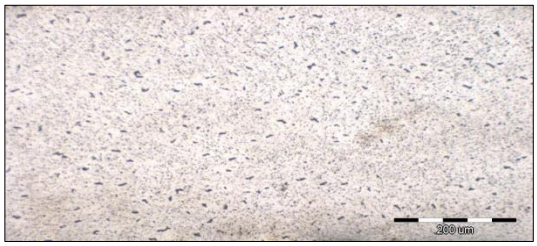

Figure 8. Zy-4 as-receive: hydrides (x100).

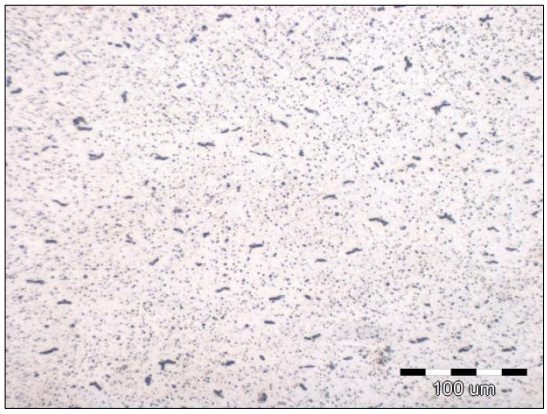

Figure 9. Zy-4 as-receive: hydrides (x200).

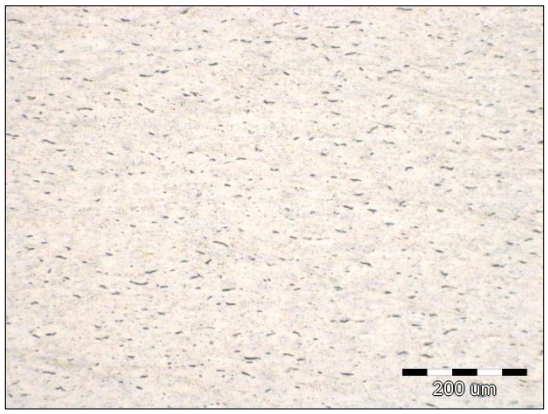

Figure 10. Zy-4_Y2-77, hydrides (x100).

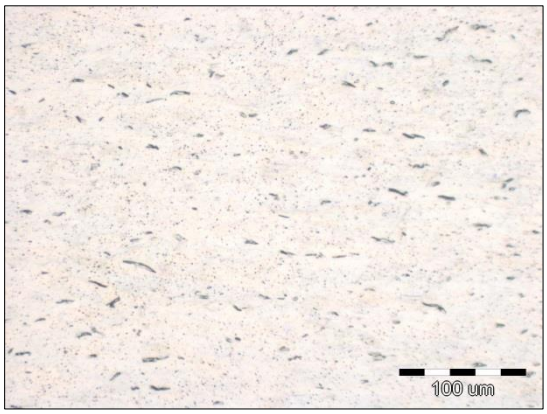

Figure 11. Zy-4_Y2-77, hydrides (x200).

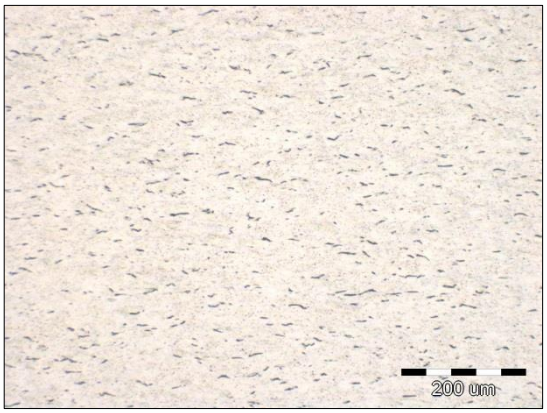

Figure 12. Zy-4 Y3-259, hydrides (x100)

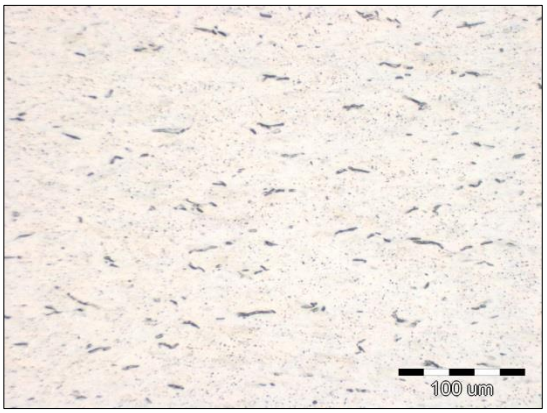

Figure 13. Zy-4 Y3-259, hydrides (x200).

3.4. X-RAYS DIFFRACTION

In the case of the Zircaloy-4 alloy, only coupon Y3-259 was investigated on the S6 support, exposed over five years in the Y3 autoclave (circuit 2 – from the circulation pump to the reactor entrance). The compounds identified on coupon Y3-259 of Zircaloy-4 in the sample volume analyzed are listed in Table 4.

Table 4. Compounds identified on Zy-4 coupons.

Chemical formula	Crystallization system	SemiQuant [%]
Zr	hexagonal	7
ZrO_2	monoclinic	17
ZrO_2	cubic	3
ZrO	cubic	11
Zr_3O	hexagonal	6
ZrO_2	monoclinic	24
$Zr_{0.936}O_2$	monoclinic	24
$ZrO_{1.98}$	tetragonal	4
Zr_3O	rhombohedral	5

It was observed that the highest weight (65%) corresponded to the monoclinic form of zirconium dioxide. The tetragonal and cubic forms of zirconium dioxide appear with very little weight in the sample volume analyzed (4% and 3%, respectively). In contrast, the cubic form of zirconium oxide was present in approximately 11% of the samples. In addition, the hexagonal and rhombohedral forms of Zr_3O oxide were highlighted.

On the surface of the Zircaloy-4 coupon, the highest weight was obtained from the monoclinic form of zirconium dioxide. The tetragonal and cubic forms of zirconium dioxide appear with very little weight in the analyzed sample volume (3-4%). In addition, the hexagonal and rhombohedral forms of Zr_3O and the cubic form of ZrO are highlighted in Fig. 14.

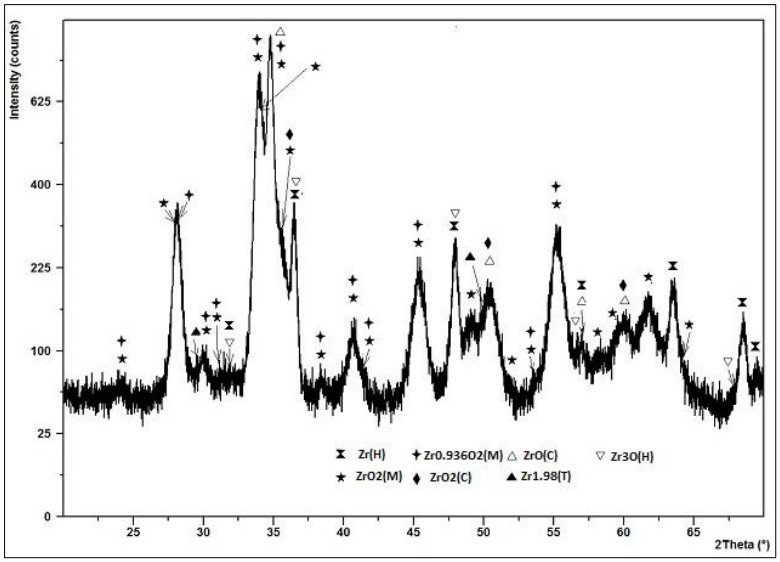

Figure 14. The diffraction spectrum corresponding to coupon 259, exposed on support S6 of autoclave Y3 - circuit 2 (from the circulation pump to the reactor inlet).

3.5. SCANNING ELECTRON MICROSCOPY SURFACE OXIDE ANALYSIS

On scanning electron microscopy, the surface of the coupons in Zircaloy-4, coupon Y2-77 (subject to the corrosion conditions specific to the cooling agent in one of the loops and whose exposure period was less than 5 years) by scanning electron microscopy at x1000 magnification, Fig. 15, showed that the formed oxide is protective, does not show cracks, exfoliation or other surface defects. Throughout the coupon surface, pores smaller than 1 μm were observed to form in or under a thin layer of oxide. In Figs 15 and 16, dark–colored deposits are observed on the surface of the oxide – identified by X-ray spectroscopy methods with energy dispersion – as carbon) and very fine nanometric crystallites are present on the surface. The small crystallites present on the surface are atypical for zirconium oxides; they can originate from the primary circuit by washing the oxides of other materials and subsequently fixing them on this coupon. Fig. 16 shows pores open on the surface, but many pores with very small nanometric dimensions were formed under the thin internal oxide substrate.

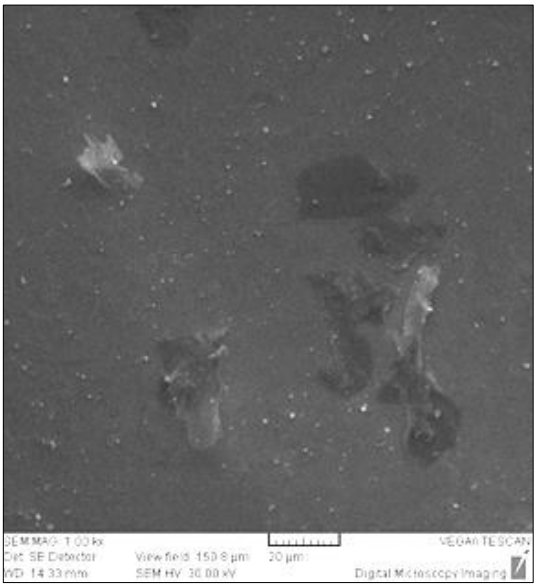

Figure 15. Surface of Zy-4 formed oxides (Y2-77).

Figure 16. Pores present on Zy-4 (Y2-77).

3.6. SCANNING ELECTRON MICROSCOPY

The images of scattered electrons taken in the cross-section of the Y2-77 coupon from Zircaloy-4 (Fig. 17) show the presence of a very small oxide layer, and the metal oxide interface is slightly corrugated. In the case of coupon Y3-259 from Zircaloy-4, Fig. 18 shows that the oxide has a small thickness, and the metal-oxide interface is slightly wavy. Very rarely, on the surface of zirconium oxide, there are deposited oxide particles brought by the cooling agent on the investigated coupon from other regions.

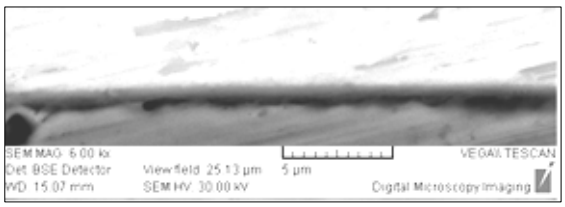

Figure 17. The oxide layer on Zy-4 sample Y2-77.

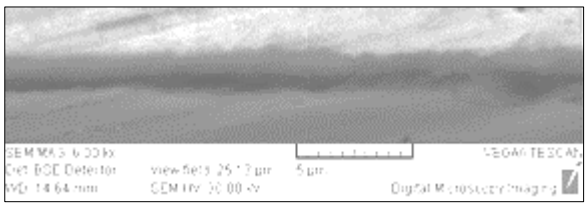

Figure 18. The oxide layer on Zy-4 sample Y3-259.

3.7. X-RAY SPECTROSCOPY WITH ENERGY DISPERSION (EDS) ANALYSIS

Regarding the Zircaloy-4 zirconium alloy, the surface deposits were examined, and from the cartographic images, it was found that the dark colored deposits (Figs. 19 and 20) were carbon, and the crystallites present on the surface were iron oxides transported by the primary agent and brought on the zirconium alloy coupons.

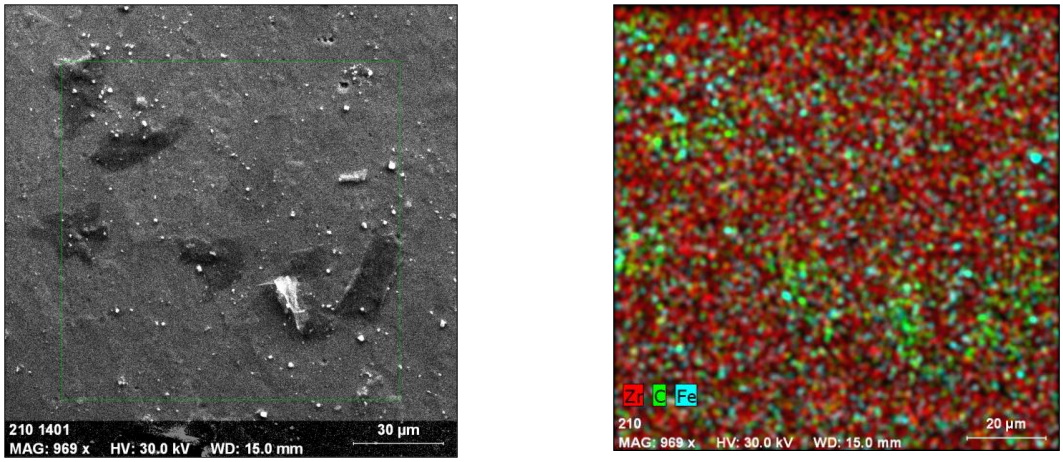

Figure 19. SEM image and EDS mapping of Fe, Zr, C on Zircaloy-4 sample - Y2-77.

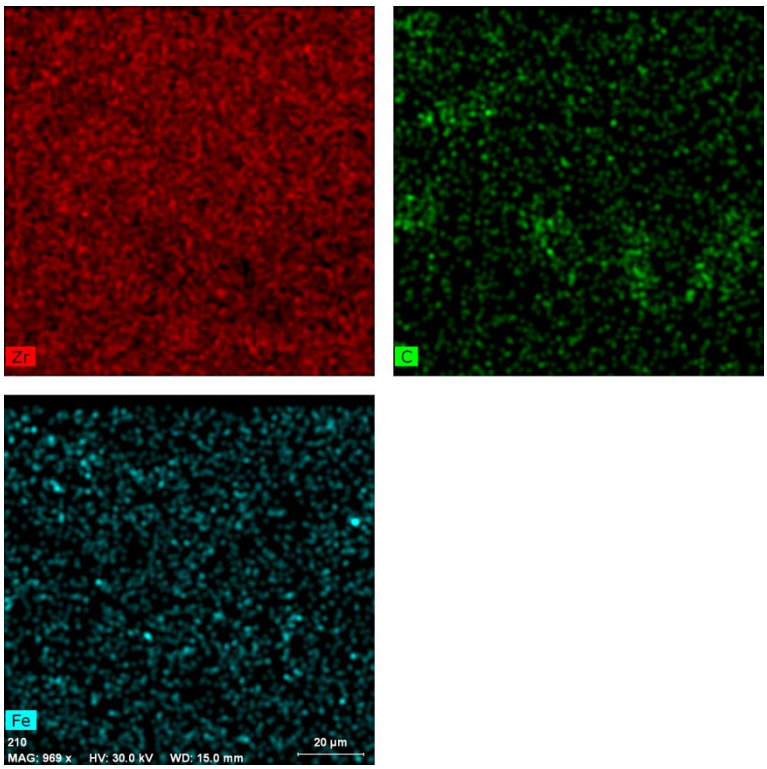

Figure 20. Elemental cartographies Fe, Zr, C on Zircaloy-4 sample Y2-77

Following the analyzes performed on the exposed Zircaloy-4 coupons tested in the autoclave System at U#1 Cernavoda NPP, it was found that the corrosion is uniform, the thicknesses of the oxide layers deposited on the surface of the coupons increase with the increase of the testing period, and the hydrides formed have a uniform distribution. The obtained results are in accordance with those reported in the specialized literature, [12, 13].

4. CONCLUSIONS

During steady-state operation of the CANDU reactor with chemical standard conditions, black and adherent magnetite crystallites, produced by the corrosion of the carbon steel feeder, precipitated from the primary coolant on the Zircaloy-4 coupons surface. The presence of these corrosion deposits on the surface did not influence the oxidation and hydriding of the Zircaloy-4 alloy.

Corrosive deposits formed under normal water chemistry conditions do not influence the oxidation or hydriding of the cladding material. The corrosion rate was approximately 0.276–0.313μm/dm^2.day, and metallographic examination evidenced the presence of uniform zirconium oxide with a thickness of 2-3μm and accelerated hydriding did not occur after approximately 2520 operation days.

The oxide layer on the coupon exposed for over 5 years is approximately 1.5 times thicker than that on the coupon exposed for less than 5 years.

The morphology of the hydrides was similar to that of the coupons tested under identical conditions from out-of-pile (laboratory) experiments.

Microstructure of Zircaloy-4 coupons: the control sample and the tested coupons have numerous hydrides per zirconium alpha structure (αZr).

Coupons exposed for over five years had the highest weight of the monoclinic form of zirconium dioxide (65%). The tetragonal and cubic forms of zirconium dioxide appear with a very small weight in the sample volume analyzed (4% and 3%, respectively). The cubic form of zirconium oxide was present in approximately 11% of the samples. In addition, the hexagonal and rhombohedral forms of Zr_3O were highlighted.

The oxides formed on Zircaloy-4 are adhesive and protective films after an operating time of less than five years. At longer exposure times (over five years), the coupons contain slightly thicker oxides, and very fine pores are formed at the metal oxide interface. This was observed on the available coupons, and there were deep traces on which iron and nickel oxides were fixed, which were transported in the autoclave.

The obtained results are useful for characterizing the corrosion behavior of Zircaloy-4 coupons exposed in the autoclave system at Cernavoda NPP for long periods.

The topic of in-situ corrosion testing for fuel cladding alloy has been the demonstration of proper and systematic aging management of the U#1 Cernavoda NPP key components, thus creating the premises for the consolidation of the Plant Life Management and Long Term Operation Program.

REFERENCES

[1] Zinkle, S.J., et al., *Journal of Nuclear Materials*, **448,** 374, 2014.
[2] Platt, P., Allen, V., et al., *Corrosion*, **98**, 1, 2015.
[3] Terrani, K.A., *Journal of Nuclear Materials,* **501,** 13, 2018.
[4] Yadav, K.K., Pal, U., Karthikeyan, R., *Nuclear and Particle Physics Proceedings*, **41**, 62, 2023.
[5] Muthu, S.M., Lee, H.B., Okonkwo, B.O., Wang, D., Jang, C., Na, T., *Materials*, **16**, 7589, 2023.
[6] Jiang, G., Xu, D., Wei, Y., Liu, H.; Liu, L., Kuang, W., *J. Chem. Eng.*, **462**, 2023.
[7] Geng, D., Deng, J., Liu, L., Sun, Q., *Journal of Nuclear Materials*, **583**, 2023.
[8] Robson, J.D., *Journal of Nuclear Materials*, **551**, 2021.

[9] Oussoren, A., Chan, P., Wowk, D., Prudi, A., *ASME J of Nuclear Rad Sci.*, **7(1),** 2021.
[10] Zotica, D., Marciulescu, O., *IAEA-TECDOC-1128, Proceedings of a Technical Committee meeting held in Hluboka nad Vltavou, Czech Republic,* **19,** 1998.
[11] Lucan, D., *International Conference on Applications of Radiation Science and Technology - ICARST, Session PA2,* IAEA, Vienna, Austria, 24–28 April, 2017.
[12] Allen, T.R., Konings, R.J.M., Motta, A.T., *Comprehensive Nuclear Materials*, **5**, 2012.
[13] Khattak, M.A., Omran, A.A.B., Kazi, S., Khan, M.S., Ali, H.M., Tariq, S.L. Akram, M.A., *Journal of Engineering Science and Technology,* **14 (3)**, 2019.